Translational Oncology
www.transonc.com

Volume 6 Number 1 February 2013 pp. 1–9 1

A Comprehensive Gene Expression Analysis of Resistance Formation upon Metronomic Cyclophosphamide Therapy[1,2]

Rebekka Kubisch*, Lilja Meissner*,[3], Stefan Krebs†, Helmut Blum†, Michael Günther*, Andreas Roidl* and Ernst Wagner*

*Pharmaceutical Biotechnology, Department of Pharmacy, Center for System-Based Drug Research, Ludwig-Maximilians University, Munich, Germany; †Laboratory for Functional Genome Analysis, Gene Center of the Ludwig-Maximilians University, Munich, Germany

Abstract

Resistance formation is one of the major hurdles in cancer therapy. Metronomic anti-angiogenic treatment of xenografted prostate cancer tumors in severe combined-immunodeficiency (SCID) mice with cyclophosphamide (CPA) results in the appearance of resistant tumors. To investigate the complex molecular changes occurring during resistance formation, we performed a comprehensive gene expression analysis of the resistant tumors *in vivo*. We observed a multitude of differentially expressed genes, e.g., *PAS domain containing protein 1*, *annexin A3* (*ANXA3*), *neurotensin*, or *plasminogen activator tissue* (*PLAT*), when comparing resistant to *in vivo* passaged tumor samples. Furthermore, tumor cells from *in vivo* and *in vitro* conditions showed a significant difference in target gene expression. We assigned the differentially expressed genes to functional pathways like axon guidance, steroid biosynthesis, and complement and coagulation cascades. Most of these genes were involved in anti-coagulation. Up-regulation of anti-coagulatory *ANXA3* and *PLAT* and down-regulation of PLAT inhibitor *serpin peptidase inhibitor clade A* were validated by quantitative real-time polymerase chain reaction. In contrast, coagulation factor F3 was upregulated, accompanied by the expression of an altered gene product. These findings give insights into the resistance mechanisms of metronomic CPA treatment, suggesting an important role of anti-coagulation in resistance formation.

Translational Oncology (2013) 6, 1–9

Introduction

Overcoming resistance to chemotherapeutic treatment is one of the major issues of clinical cancer research nowadays. Up to now, a variety of molecular mechanisms leading to chemoresistance of cancer cells has been investigated and new treatment strategies have been developed. Besides targeted therapy and combinatorial treatments, anti-angiogenic therapy is another promising option to circumvent resistance formation. For example, in prostate cancer, the prognosis for patients with hormone-resistant prostate carcinoma is poor, because of frequent chemoresistance that is often followed by relapse and further tumor progression [1,2]. One suggested follow-up therapy for taxane-resistant hormone-resistant prostate carcinoma is the metronomic treatment with cyclophosphamide (CPA), reviewed by Emmenegger et al. [3].

The alkylating agent CPA, if given in normal dose, preferably targets tumor cells. However, if frequent administration of low dose is carried out (metronomic therapy), it acts as an anti-angiogenic drug, as reviewed by Kerbel and Kamen [4].

The pivotal targets of anti-angiogenic therapy are not cancer cells but blood vessels, supplying the tumor with nutrients and oxygen. Thus, one advantage of anti-angiogenic therapy is that it targets endothelial cells not carrying a malignant phenotype. These cells are not able to develop resistance to the treatment, like cancer cells do, due to their genetic instability.

Address all correspondence to: Rebekka Kubisch, Diploma or Ernst Wagner, PhD, Pharmaceutical Biotechnology, Department of Pharmacy, Center for System-Based Drug Research, Ludwig-Maximilians University, Butenandtstr. 5-13, 81377 Munich, Germany. E-mail: rebekka.kubisch@cup.uni-muenchen.de, ernst.wagner@cup.uni-muenchen.de

[1]We are grateful to the EU project GIANT and Nanosystems Initiative Munich for funding.

[2]This article refers to supplementary materials, which are designated by Tables W1 to W8 and Figures W1 to W4 and are available online at www.transonc.com.

[3]Present address: Institute for Stroke and Dementia Research, University of Munich Medical Center Grosshadern, Ludwig-Maximilians University, Munich, Germany.

Received 28 August 2012; Revised 18 December 2012; Accepted 24 December 2012

DOI 10.1593/tlo.12295

Studying the mechanisms leading to resistance to anti-angiogenic therapy is of great interest, as they may differ from resistance to classic chemotherapy.

Resistance to anti-angiogenic therapy can be classified into four major groups: 1) evasive resistance, 2) vascular cooption, 3) reduced vascular dependence, and 4) vascular remodeling [5].

In 2011, Emmenegger et al. pointed out that the applied CPA dose (maximum dose or metronomic) directly changes the mechanisms of resistance formation. After treatment of PC3 xenografts with maximum dose, tumor cells acquired resistance *in vivo* and *in vitro* [5]. However, after metronomic application of CPA, the resistant phenotype became manifested only *in vivo*.

Thoenes et al. showed that metronomic CPA therapy of prostate cancer xenografts has an anti-angiogenic effect. Tumor vessels were destroyed and blood supply was reduced during the treatment. Tumors developed a resistance to the therapy regimen without restoring tumor vessels or vascular mimicry [6]. Isolated tumor cell lines from resistant tumors revealed their resistant phenotype only upon reimplantation *in vivo* but remained sensitive to chemotherapy in cell culture. In this particular study, a comparative proteome analysis of chemoresistant *versus* parental PC3 cells was performed, suggesting the involvement of the coagulation inhibitor annexin A3 (ANXA3) [6]. However, a genome-wide screen of tumors under the far more relevant *in vivo* conditions had not yet been performed.

The current study elucidates genetic alterations of CPA-induced tumor resistance *in vivo* using a microarray-based approach.

Materials and Methods

Cell Culture

Cell culture media, antibiotics, FBS, and trypsin/EDTA solution were purchased from Invitrogen/Life Technologies (Carlsbad, CA). PC3 human prostate carcinoma cells (PC3-wt, ATCC #CRL1435) and reisolated clones PC3 A3, PC3 D3, and PC3 D4 were cultured in RPMI 1640 medium supplemented with 10% FBS. Cells were grown at 37°C in 5% CO_2 in a humidified atmosphere. Generation of these PC3 cell lines was previously described by Thoenes et al. [6]. Briefly, standard PC3 cells (PC3-wt) had been injected into male severe combined-immunodeficiency (SCID) mice and treated with a metronomic regimen of CPA (120 mg/kg every 6 days). After a response phase, tumors restarted growing. Cells of two different resistant tumors were isolated (PC3 D3 and PC3 D4). Additionally, a cell line of untreated tumors was established (PC3 A3), representing an *in vivo* passaged control cell line [6]. PC3 subclones were cultured without antibiotics for at least three to four passages before tumor cell implantation and were harvested when reaching approximately 70% confluence.

In Vivo *Experiments*

Male SCID mice (CB17/lcr-PrkdcSCID/Crl; 8–10 weeks) were housed in individually ventilated cages, under specific pathogen-free conditions, with a 12-hour day/night cycle and food and water *ad libitum*. For tumor formation, 1×10^6 cells in 100 µl of phosphate-buffered saline were injected subcutaneously with a 25-G needle (Braun) into the flank of SCID mice (five animals per group). PC3-wt, PC3 A3, PC3 D3, and PC3 D4 cells were injected and grown as xenografts until they reached a mean volume of 30 mm^3. One group of each PC3 subclone was treated intraperitoneally with 120 mg/kg CPA (Sigma-Aldrich, St Louis, MO). At 24 hours after CPA application, tumors were harvested (for experimental overview, see Figure W1). Four individual tumors of each group (PC3-wt, PC3 A3, PC3 D3, and PC3 D4) were analyzed in a microarray experiment [i.e., four human Gene Chip gene 1.0 ST arrays (Affymetrix, Santa Clara, CA) per group]. All animal procedures were approved and controlled by the local ethics committee and carried out according to the guidelines of the German law of protection of animal life.

Microarray

Total RNA was isolated from tumor samples using a tissue homogenizer (Silent Crusher M, Heidolph, Germany) and the TRIzol method. Total RNA was checked for purity and integrity (ND-1000; Thermo Fisher Scientific, Waltham, MA and Bioanalyzer 2100; Agilent Technologies, Santa Clara, CA), and 100 ng was used for preparation of labeled probes for microarray hybridization. For this purpose, Affymetrix-cDNA synthesis and amplification and terminal labeling kits were used according to the manufacturer's instruction. Briefly, total RNA was reversely transcribed into cDNA using T7 promoter–tagged random primers; cDNA was amplified by *in vitro* transcription and again reverse transcribed. The resulting cDNA was fragmented, terminally labeled, and finally hybridized to Affymetrix GeneChips (HuGene 1.0 ST arrays, Affymetrix) and scanned on an Affymetrix GeneChip Scanner 3000.

Data analysis

Raw data were read into the statistical software R [7] and normalized by the robust multichip analysis (RMA) method [8] within the xps package from Bioconductor [9]. Differentially expressed genes and scatter plots were generated using the program spotfire (TIBCO). *P* values were calculated using the analysis of variance test, and adjusted *P* values were calculated with R using the false discovery rate method. Functional analysis was performed using Database for Annotation, Visualization and Integrated Discovery (DAVID) Functional Annotation Bioinformatics Microarray Analysis [10]. The description by Huang et al. [10] specifies the stated *P* value as the threshold of EASE score, a modified Fisher Exact *P* value, for gene enrichment analysis. It ranges from 0 to 1. Fisher Exact *P* value = 0 represents perfect enrichment. Usually, the *P* value is equal or smaller than .05 to be considered strongly enriched in the annotation categories.

To determine the species specificity of each microarray, we mapped all oligonucleotides from the HuGene 1.0 ST array to the mouse Refseq transcriptome using the ngs mapper Bowtie. We obtained no perfectly matching hits, only 23 probes with a single mismatch and 130 probes with two mismatches. 25mers with three or more mismatches were regarded as not contributing to the measured signal in a cross-species context. None of the genes that were differentially expressed had any oligonucleotide probes that could be mapped to the mouse transcriptome. Thus, we conclude that the results are not affected by cross-hybridization of host-derived transcripts.

For the identification of alternative splicing, a filtering approach was used. First, the splice index was calculated by the MiDAS program from Affymetrix apt package. Then, genes were plotted on probe level together with the gene model to verify alternative splicing by visual inspection.

Quantitative Real-Time Polymerase Chain Reaction

Total RNA was isolated using NucleoSpin RNA Isolation Kit (Macherey-Nagel, Dueren, Germany) and transcribed with the Transcriptor High Fidelity cDNA Synthesis Kit (Roche Diagnostics, Risch, Switzerland) according to manufacturers' protocols. Quantitative

real-time polymerase chain reaction (qPCR) was performed using UPL Probes (Roche) and Probes Master (Roche) on a LightCycler 480 System (Roche) with *glyceraldehyde 3-phosphate dehydrogenase* (*GAPDH*), *β-actin*, and *B2M* as control.

Human primers used include:

β-actin (UPL Probe #64), left: ccaaccgcgagaagatga, right: ccagaggcgtacagggatag;
ANXA3 (UPL Probe #29), left: tccggaaagctctgttgact, right: atcttgtttggccagatgct;
B2M (UPL Probe #42), left: ttctggcctggaggctatc, right: tcaggaaatttgactttccattc;
bone morphogenetic protein receptor type 1B (BMPR1B; UPL Probe #21), left: tttcatgccttgttgataaaggt, right: gcttgtttaacttttgtttcctctc;
dehydrogenase/reductase member 2 (DHRS2; UPL Probe #4), left: tgagactatcacctatcgccaag, right: cagcatagtggttggtgtctg;
F3 exons 1and 2 (UPL Probe #15), left: cgccaactggtagacatgg, right: gctgccacagtatttgtagtgc;
F3 exons 5 and 6 (UPL Probe #2), left: cagacagcccggtagagtgt, right: ccacagctccaatgatgtagaa;
GAPDH (UPL Probe #60), left: ctctgctcctcctgttcgac, right: gcccaatacgaccaaatcc;
Neurotensin (NTS; UPL Probe #17), left: cagcttgtatgcatgctactcc, right: aatgctttcatttcctcttctga;
PAS domain containing protein 1 (PASD1; UPL Probe #20), left: caacccacctaccatcaggt, right: ctgctccgcagat ctcatc;
plasminogen activator tissue (PLAT; UPL Probe #59), left: cgggtggaatattgctggt, right: cttggctcgctgcaactt;
protein Sα (PROS1; UPL Probe #46), left: acatacctgggtggccttc, right: tccagatccaactgtacaccat;
special AT-rich sequence-binding protein-1 (SATB1; UPL Probe #44), left: aatggcattgctgtctctagg, right: actttccaacctggattagcc;
serpin peptidase inhibitor clade A, member 1 (SERPINA1; UPL Probe #73), left: gcttaaatacggacgaggaca, right: acgagacagaagacggcatt;
serpin peptidase inhibitor clade D, member 1 (SERPIND1; UPL Probe #29), left: tggtggagagatggcaaaa, right: gattgtagttcttctccagcttgaat;
serine peptidase inhibitor clade B, member 7 (SERPINB7; UPL Probe #8), left: gattgtagttcttctccagcttgaat, right: caaattgaacttccgttcctg.

Experiments were done in triplicates and the obtained average C_T values of target genes were normalized to control as ΔC_T. Changes in expression levels were shown as fold expression ($2^{-\Delta\Delta CT}$), calculated by the $\Delta\Delta C_T$ method [11].

Western Blot

After sodium dodecyl sulfate–polyacrylamide gel electrophoresis and transfer to a nitrocellulose membrane (Bio-Rad Laboratories, Hercules, CA), the blot was probed with either a goat polyclonal antibody detecting tissue factor (F3) (1:1000; Santa Cruz Biotechnology, Inc, Santa Cruz, CA) or with a rabbit monoclonal antibody detecting GAPDH (1:1000; Cell Signaling Technology, Inc, Cambridge, United Kingdom) in Tris-buffered saline containing 0.5% Tween and 5% nonfat milk powder at 4°C overnight. After washing with Tris-buffered saline containing 0.5% Tween, the membranes were exposed to horse anti-goat HRP-conjugated secondary antibody (1:10,000; Vector Laboratories, Burlingame, CA) or a mouse anti-rabbit HRP-conjugated secondary antibody (1:10,000; Vector Laboratories) followed by a chemiluminescence detection (LumiLight; Roche Diagnostics).

Results

Comprehensive Analysis of Differentially Expressed Genes

To analyze the gene expression of chemoresistant tumor tissue, a genome-wide microarray of xenografted PC3 tumor cell lines PC3

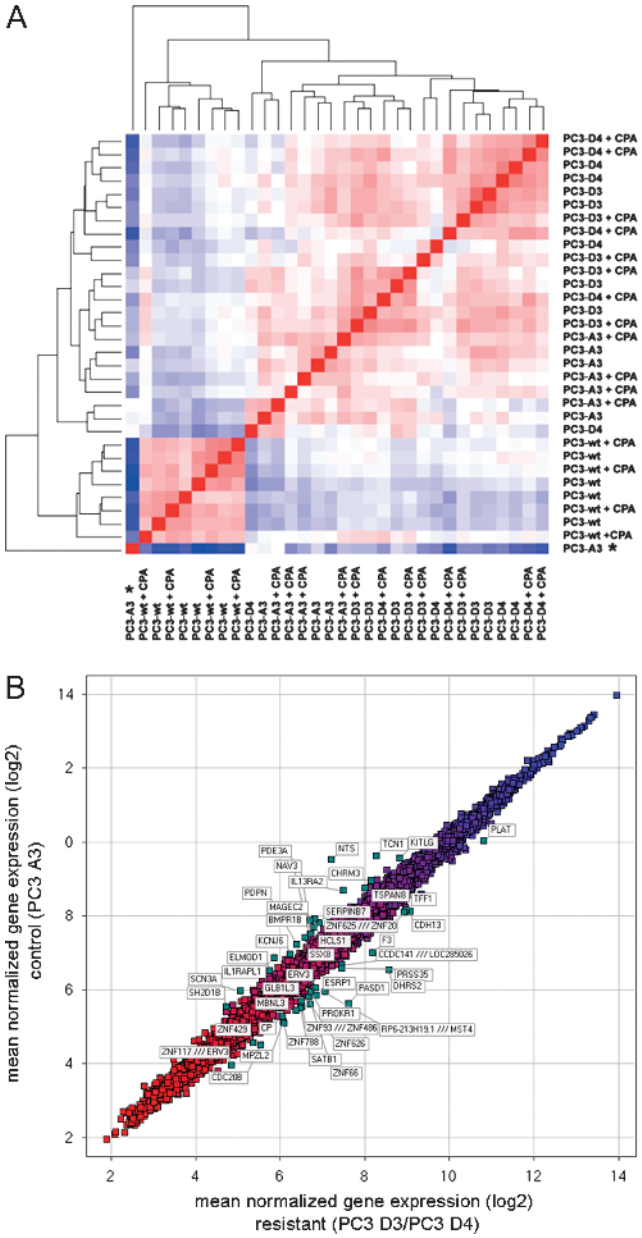

Figure 1. Gene expression of the resistant tumors PC3 D3 and PC3 D4. (A) Hierarchical clustering on RMA normalized arrays (four tumors per group). Red, low distance; blue, high distance. Outliners, marked by an asterisk, are excluded from further data analysis. (B) Scatter plot of mean normalized gene expression ($\log_2$) PC3 D3/PC3 D4 *versus* PC3 A3. (C) Venn diagram of PC3 D4 *versus* A3 and PC3 D3 *versus* A3 differentially expressed genes (cutoff = 0.4 relative expression change) and table including the top 10 of genes differentially expressed by both PC3 D3 and PC3 D4. Bold, qPCR-validated genes. (D) Validation of differentially expressed genes by qPCR (fold expression to control PC3 A3): *DHRS2*, *PASD1*, *SATB1 homeobox 1* (SATB1), *NTS*, and *BMPR1B*. *$P < .05$, **$P < .005$, ***$P < .0005$ (*t* test).

D3 and PC3 D4, carrying an *in vivo* resistant prostate cancer genotype, was performed. The four PC3 sublines PC3-wt (standard PC3 cells, *in vitro* cell culture), PC3 A3 (*in vivo* passaged control cells), and *in vivo* resistant cells PC3 D3 and PC3 D4 were injected subcutaneously into SCID mice (for generation of resistant and control sublines, see Materials and Methods section). After tumor formation, one group of each PC3 subline was treated with CPA, whereas the other group was kept untreated. Microarray analysis of four individual tumors per group was performed using human Gene Chip gene 1.0 ST arrays (for an overview, see Figure W1).

To detect distances and similarities between different samples, RMA normalized data were subjected to hierarchical clustering. Here, we observed distinct clustering of the different cell lines. In contrast, acute CPA treatment of the different tumors did not induce additional clusters (Figure 1*A*). Even though this indicates only a minor direct effect of CPA on the gene expression profile, we depict the scatter plots of differentially expressed genes under direct CPA influence in Figure W2, *A* to *C*, and summarized the differential expressed genes in Tables W4 to W6. The resistant tumor sublines PC3 D3 and PC3 D4 showed a close relation of their gene expression profile, suggesting a similar resistance

C

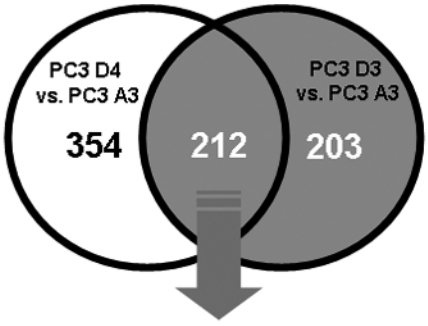

up regulated				down regulated			
Transcript Cluster ID	**Gene Symbol**	**fold expression**	**p-value (ANOVA)**	**Transcript Cluster ID**	**Gene Symbol**	**fold expression**	**p-value (ANOVA)**
7973433	**DHRS2**	**2.02**	**0.00000032**	7898057	PDPN	-0.86	0.00026646
8170488	**PASD1**	**1.98**	**0.00000008**	**8021623**	**SERPINB7**	**-0.91**	**0.02653295**
7917875	**F3**	**1.16**	**0.05352322**	**8096511**	**BMPR1B**	**-0.92**	**0.00024335**
8169949	RP6-213H19.1	1.10	0.00110133	8056376	SCN3A	-0.93	0.00194107
8035795	ZNF626	1.09	0.00004049	8166593	IL1RAPL1	-1.03	0.00030803
8112053	CDC20B	1.02	0.00004346	8089911	HCLS1	-1.12	0.00000481
8147351	ESRP1	1.00	0.00004638	8175562	MAGEC2	-1.19	0.00128070
8025992	ZNF788	0.96	0.00000139	8174598	IL13RA2	-1.22	0.00278847
8085716	**SATB1**	**0.96**	**0.00000496**	7948444	TCN1	-1.38	0.00001062
7997504	CDH13	0.95	0.00000309	**7957458**	**NTS**	**-2.34**	**0.00001741**

D

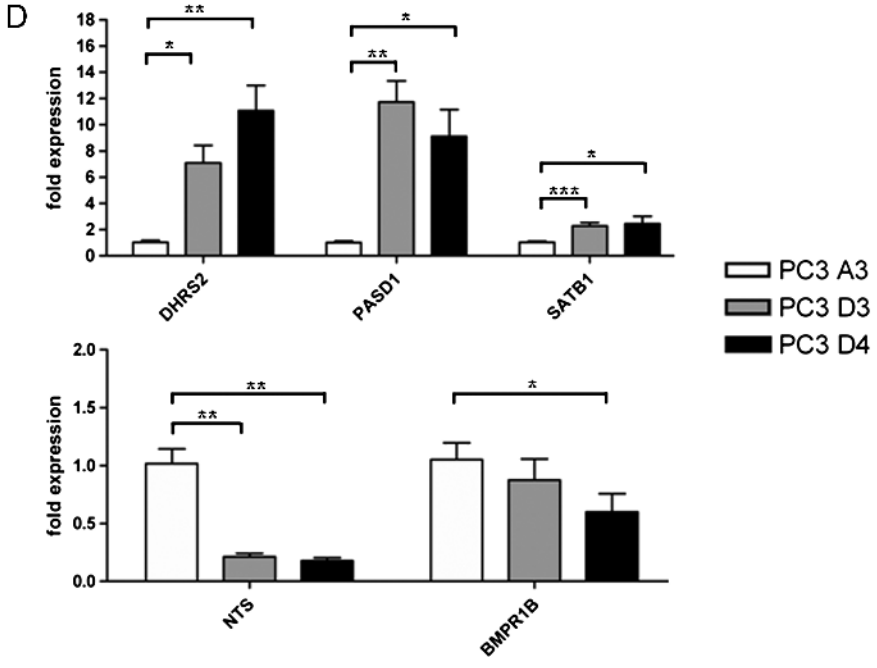

Figure 1. (*continued*).

A

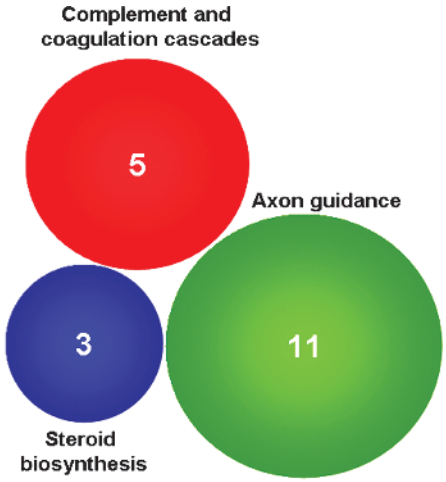

Term	Count	%	p-Value
Axon guidance	11	3.4	0.00019
Steroid biosynthesis	3	0.9	0.04298
Complement and coagulation cascades	5	1.5	0.04605

B

Transcript Cluster ID	Gene Symbol	Gene Title	fold expression	p-value (ANOVA)
7917875	F3	coagulation factor III (thromboplastin, tissue factor)	1.16	0.053523
8150509	PLAT	plasminogen activator, tissue	0.77	0.000282
8095986	ANXA3	annexin A3	0.44	0.023838
8089015	PROS1	protein S (alpha)	-0.46	0.002819
8071420	SERPIND1	serpin peptidase inhibitor, clade D (heparin cofactor), member 1	-0.55	0.002667
7981068	SERPINA1	serpin peptidase inhibitor, clade A (alpha-1 antiproteinase, antitrypsin), member 1	-0.72	0.000050
8021623	SERPINB7	serpin peptidase inhibitor, clade B (ovalbumin), member 7	-0.91	0.026533

Figure 2. (A) KEGG pathway analysis of differentially expressed genes (cutoff = 0.4 relative expression change). (B) Overview of fold expression of coagulation pathway–associated genes.

genotype. Furthermore, *in vivo* passaging strongly influenced the gene expression profile. When comparing PC3-wt, the *in vitro* passaged subline, with PC3 A3 (*in vivo* passaged), we found, for example, *ceruloplasmin* strongly downregulated. In contrast *reelin*, an extracellular matrix serine protease, is one of the upregulated genes, demonstrating the influence of the tumor environment *in vivo* (Figure W2*D* and Tables W7 and W8).

Further analyses were focused on the inherent differences between samples of resistant cell lines PC3 D3 and PC3 D4 *versus in vivo* passaged cell line PC3 A3 without the direct influence of CPA. A scatter plot of the mean of the normalized gene expression of PC3 D3 and PC3 D4 *versus* PC3 A3 shows the 50 most differentially expressed genes (Figure 1*B*).

Analysis of PC3 D3 *versus* PC3 A3 and PC3 D4 *versus* PC3 A3 revealed 415 differentially expressed genes for PC3 D3 and 566 for PC3 D4. An intersecting set of 212 genes was differentially expressed in both resistant tumor lines (Figure 1*C* and Table W1). The most differentially regulated genes *DHRS2*, *PASD1*, and *NTS* as well as resistance-related genes like *SATB1* and *BMPR1B* were chosen for further analysis. The expression of *DHRS2*, *PASD1*, and *SATB1* was increased in the resistant tumors compared to PC3 A3 tumors, whereas *NTS* and *BMPR1B* expression was decreased in resistant tissue.

Validation by qPCR confirmed all five genes as differentially expressed (Figure 1*D*). *DHRS2* had a 7.1-fold increased expression level in PC3 D3 and 11.1-fold in PC3 D4 compared to PC3 A3. *PASD1* showed an expression change of 11.7-fold in PC3 D3 and 9.1-fold in PC3 D4 compared to PC3 A3. Additionally *SATB1* showed higher expression levels in PC3 D3 (2.4-fold) and PC3 D4 (2.3-fold). Expression of *NTS* was clearly reduced in resistant sublines, PC3 D3 and PC3 D4 (five-fold). In contrast, *BMPR1B* expression was significantly decreased only in PC3 D4 samples.

To evaluate the *in vivo versus* the *in vitro* expression, we analyzed these five genes under cell culture conditions. Comparing the results, the *in vitro* expression clearly differed from the *in vivo* expression of all five genes (Figure W3).

Analysis of Involved Pathways

To identify which pathways might be involved in resistance formation, a Kyoto Encyclopedia of Genes and Genomes (KEGG) pathway analysis was performed using DAVID Functional Annotation Bioinformatics Microarray Analysis [10]. This method revealed a potential involvement of the following three pathways: 1) axon guidance, 2) steroid biosynthesis, and 3) complement and coagulation cascades (Figure 2*A*).

As blood flow might play a crucial role during resistance formation to anti-angiogenic therapy, further analysis was focused on the genes grouped in complement and coagulation cascades. The expression of *F3*, *PLAT*, and *ANXA3* was increased in the resistant tumors, whereas

the expression of *PROS1*, *SERPIND1*, *SERPINA1*, and *SERPINB7* was decreased (Figure 2*B*). Additionally, the two differentially expressed coagulation genes *ANXA3* and *SERPINB7* were added to this group, although their regulation was below the cutoff.

Gene Expression of Coagulation-Related Genes Is Modulated in Resistant Tumors

qPCR analysis of these coagulation-related genes confirmed the gene expression profiles obtained by microarray analysis. First, we analyzed the mRNA expression of the coagulation-promoting proteins. The coagulation-promoting genes *SERPINA1*, *SERPIND1*, *SERPINB7*, and *PROS1* were downregulated in resistant tumors. In contrast, the expression level of *F3* was slightly increased in PC3 D3 tumor tissue and displayed a very high expression in PC3 D4 tumor tissue.

Moreover, mRNA expression of proteins hampering coagulation (PLAT and ANXA3) was increased in PC3 D3 and PC3 D4 tumor tissue compared to PC3 A3 control tissue (Figure 3*A*).

When analyzing the gene expression of *in vitro* cultured cell lines, we observed a different pattern. *F3*, *PLAT*, and *ANXA3* showed no altered gene expression in PC3 D3 and PC3 D4 *versus* PC3 A3, whereas the expression profile of *SERPINA1*, *SERPIND1*, *SERPINB7*, and *PROS1* were similarly downregulated *in vivo* (Figure 3*B*).

Taken together, genes that encode anti-coagulation proteins were upregulated and genes that code for proteins promoting coagulation were downregulated, except *F3*, in resistant tumor tissue compared to

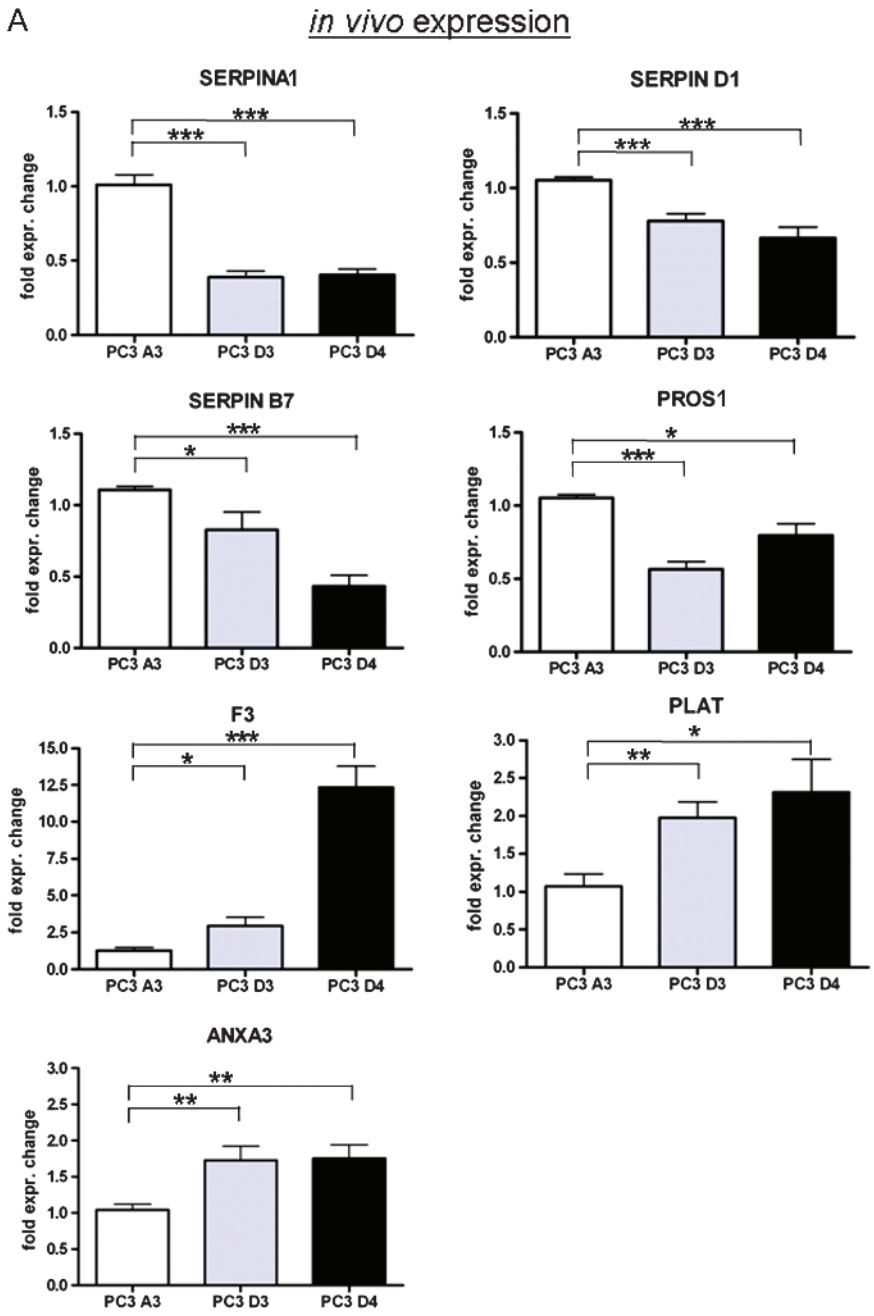

Figure 3. (A) Validation of coagulation-related genes by qPCR (fold expression to control PC3 A3). (B) Expression of coagulation-related genes *in vitro* analyzed by qPCR. *$P < .05$, **$P < .005$, ***$P < .0005$ (*t* test).

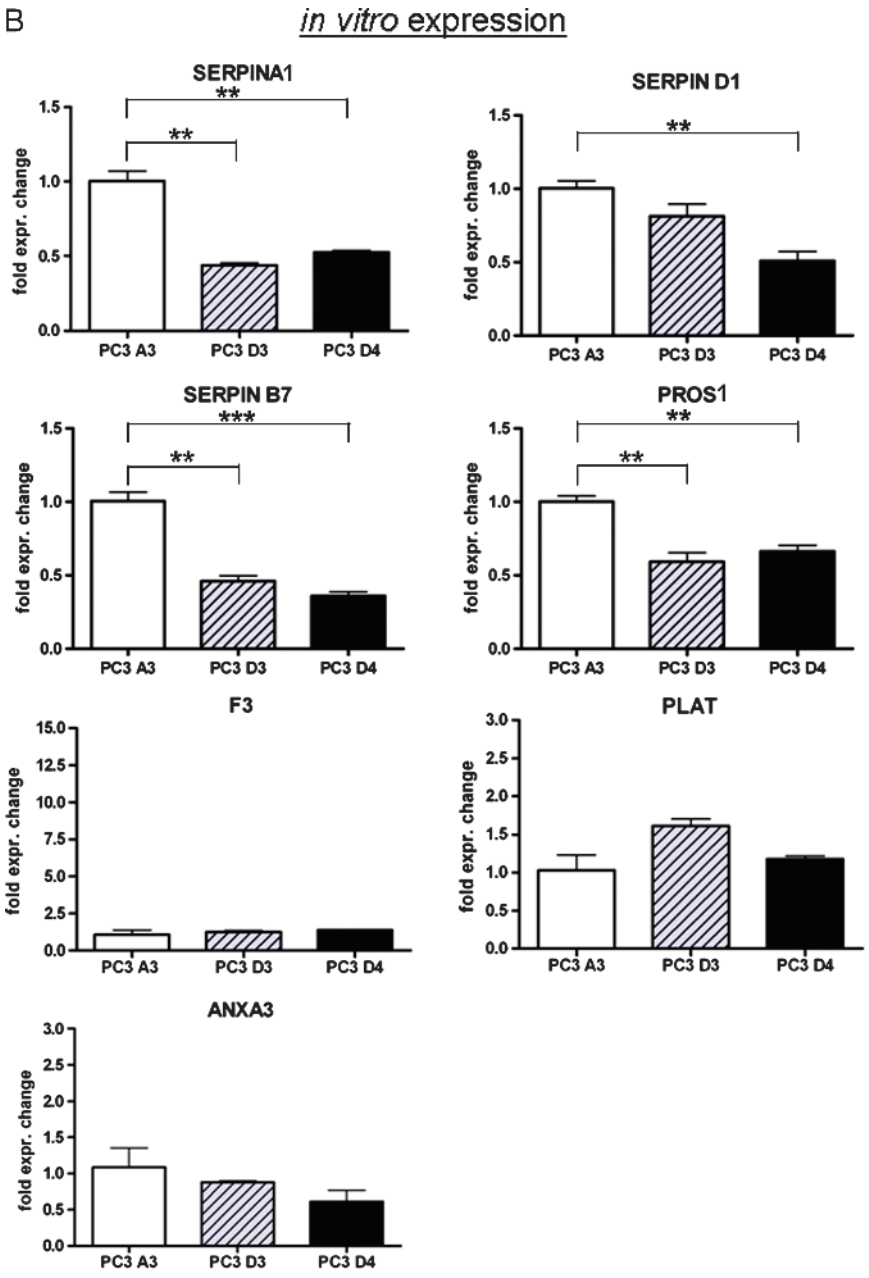

Figure 3. (*continued*).

in vivo passaged control tumors. However, these effects are not present *in vitro*.

F3 Exon Structure Is Altered in Resistant PC3 D4 Tumors

F3 is the only candidate that does not fit into the picture of an anti-coagulative signature in resistant tumors, as it is a coagulation-promoting gene and highly upregulated in resistant tumor tissue (34-fold). Therefore, we had a closer look at the exon structure of F3. The microarray probe setup allowed us to analyze the expression of a single exon in detail. Comparing resistant PC3 D4 to *in vivo* passaged control PC3 A3 tissue, the exon expression profile of F3 shows an altered signal intensity between exons 3 and 6 (Figure 4*A*), whereas no differences were detected in exons 1 and 2. This indicates the expression of different *F3* isoforms. Sequencing of the *F3* gene transcript revealed no mutations in the coding sequence (data not shown). We hypothesized that two different transcripts of the *F3* gene are present, one being prominently expressed in PC3 D4 tumors.

Thus, we analyzed the expression levels of exons 1 and 2 and exons 5 and 6, respectively. In PC3 D4, we observed a higher relative expression of exons 5 and 6 compared to exons 1 and 2, providing evidence for the presence of two different *F3* transcripts (Figure 4*B*). Western blot analysis of the F3 protein expressed by PC3 D4 cell line when cultured *in vitro* compared to samples from tumor tissue reflects the qPCR results. *In vitro* PC3 D4 cells express low levels of F3 protein with a molecular weight of 47 kDa. On the contrary, in PC3 D4 tumor samples, two types of F3 protein were observed, one with 47 kDa and another one with a lower molecular weight. The smaller F3 form is more abundant than the 47-kDa form (Figure 4*C*). Overall, we hypothesize the additional presence of a short form of F3 missing exons 1 and 2 in resistant tumors *in vivo*. The loss of these exons might lead to an altered protein function, helping to maintain the anti-coagulative status.

Discussion

Cells developing resistance to metronomic CPA therapy undergo a complex molecular evolution. Changes in many different factors and pathways contribute to the formation of a resistant phenotype. As shown earlier, most of the classic resistance mechanisms can be ruled out in this study, as neither increased multi-drug resistance (MDR) transporter activity nor neoangiogenesis, vascular mimicry, or impaired CPA activation was observed [6]. A pharmacodynamic study of metronomically administered CPA suggests that it is unlikely that resistance to this kind of regimen is caused by impaired CPA activation [12].

One of the four different categories of resistance to anti-angiogenic therapy is "reduced vascular dependence." As shown previously, this resistance mechanism applies here, as the resistant tumor grows under conditions of hypoxia and restricted nutrients without the formation of additional tumor vessels [6]. To investigate the molecular basis of this *in vivo* resistance mechanism to anti-angiogenic CPA therapy, a genome-wide microarray was performed. This study clearly shows that it is important to use appropriate *in vivo* controls, as already the comparison of the gene expression profile of *in vivo* passaged and standard PC3 tumors (PC3-wt) displayed a dramatic difference. The gene expression profile of the standard PC3-wt samples was clearly distinct from all other *in vivo* passaged tumor sublines (Figure 1*A*).

Moreover, gene expression of resistant tumors PC3 D3 and PC3 D4 clearly differed from passaged non-resistant PC3 A3 tumors. An acute CPA treatment of the respective tumors for 24 hours only influenced gene expression marginally (Figure 1*A*). All PC3 D3 samples from four mice clustered in one group, distinct from the PC3 D4 group. Approximately 50% of the differentially expressed genes in PC3 D3 and PC3 D4 *versus* PC3 A3 were shared by both resistant sublines (Figure 1*C*). To rule out clonal variation instead of chemoresistance as cause of the observed differences, we performed a control experiment. Here, we compared the initial experiment of PC3 D3 and PC3 D4 *versus* PC3 A3 to the control experiments PC3 A3 and PC3 D3 *versus* PC3 D4 as well as PC3 A3 and PC3 D4 *versus* PC3 D3 (see Figure W4, *A* and *B*). We could identify less than 2.7% of the genes to be commonly regulated. Therefore, we regard the signature of resistant genes as considerable.

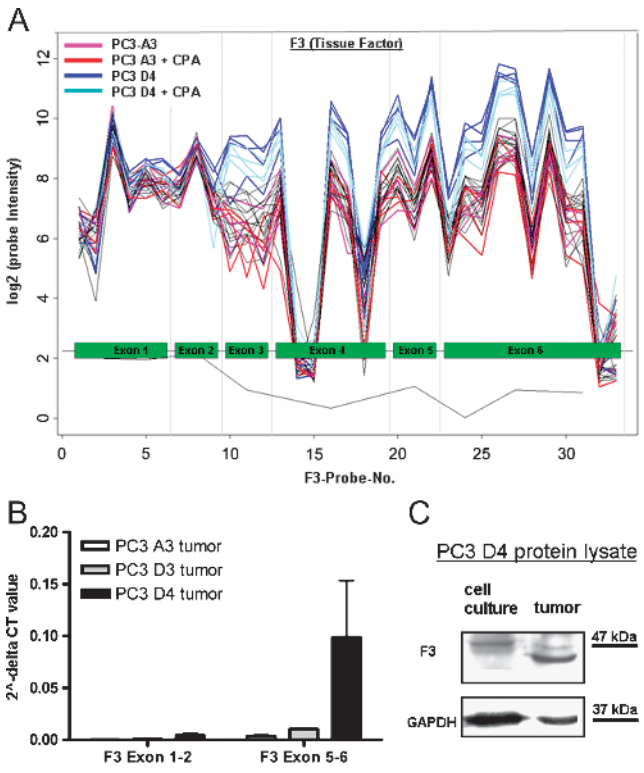

Figure 4. (A) Microarray expression profile (probe intensity) of *F3* (*tissue factor*). (B) qPCR of exons 1 and 2 and exons 5 and 6 of F3. (C) Western blot analysis of F3 in resistant cell line PC3 D4 from *in vitro* cell culture samples and *in vivo* tumor samples.

Taken together, we assume that not a single main mechanism is present in the resistant cell lines but more likely a complex molecular evolution, leading to the ability to survive the restrictive conditions of anti-angiogenic therapy.

In our model, expression of resistance-related genes *in vivo* differs from gene expression *in vitro*, indicating an involvement of microenvironmental factors leading to the observed *in vivo* resistance. The following three pathways that potentially contribute to the resistant phenotype were identified: 1) axon guidance, 2) steroid biosynthesis, and 3) complement and coagulation cascades (Figure 2*A*). As prostate cancer cells are able to gain neuronal properties [13,14], neuroendocrine-like differentiation might take place as a side effect of resistance formation. Steroid synthesis might be altered leading to hormone-promoted increased proliferation.

The most interesting functional group is "complement and coagulation cascades." This group consists of six differentially expressed genes that are associated with the coagulation cascade. During anti-angiogenic treatment, blood vessels are destroyed and coagulation takes place. In mice, the administration of flavone acetic acid, an anti-angiogenic drug, strongly reduces the coagulation time [15]. We speculate that resistant tumor cells hamper the coagulation process to overcome the reduced oxygen and nutrient supply: 1) PLAT (reviewed in [16]) and 2) ANXA3 [17] showed increased expression in resistant tumors, whereas expression of pro-coagulation gene *PROS1* (reviewed in [18]) and three members of the serine protease inhibitor family, 1) *SERPINA1*, 2) *SERPINB7*, and 3) *SERPIND1*, were decreased in resistant tumor tissue. Increased diffusion of oxygen and nutrients is facilitated by impaired thrombosis and fibrosis. Additionally, metronomic dosing of an inhibitor of systemic vasculogenesis was reported to cause increased blood flow in luciferase-tagged LM2-4 tumor xenografts [19].

In contrast to our finding that the expression of anti-coagulation genes is increased and that of pro-coagulation genes is decreased, F3, the main mediator of the extrinsic pathway of blood coagulation [20,21], was highly expressed in PC3 D4 tumor tissue. Interestingly, *F3* shows an altered exon expression profile in PC3 D4 tumor samples. Comparing expression of PC3 D4 to PC3 A3, exons 3 to 6 are highly expressed in resistant PC3 D4 tumor tissue, whereas no differential expression of exons 1 and 2 can be seen. A version of *F3*, missing exons 1 and 2, has not yet been described, whereas an alternatively spliced variant of F3, missing exon 5, has been reported [22]. Exons 1 and 2 of *F3* are coding for the first 70 amino acids of the protein. In this area, according to UniProt database [23], a signal peptide and parts of a topological domain are located. Thus, we speculate that the expression of an altered F3 protein might result in an impaired activation of blood coagulation by resistant tumor tissue or even in facilitating blood flow. Such a hypothesis, however, remains to be verified by future studies.

In conclusion, resistance formation to metronomic CPA therapy can be seen as a molecular evolutionary process. Anti-coagulation properties of the cells (increased *PLAT* and *ANXA3*, increased exon deletion variant of F3, and decreased *PROS1*, *SERPIND1*, *SERPINA1*, and *SERPINB7*) could be part of a complex resistance mechanism. The functional relevance remains to be confirmed by subsequent studies.

Acknowledgments

We thank Alexander Graf for his help with the statistical analysis in R.

References

[1] Oudard S, Banu E, Beuzeboc P, Voog E, Dourthe LM, Hardy-Bessard AC, Linassier C, Scotte F, Banu A, Coscas Y, et al. (2005). Multicenter randomized phase II study of two schedules of docetaxel, estramustine, and prednisone versus mitoxantrone plus prednisone in patients with metastatic hormone-refractory prostate cancer. *J Clin Oncol* **23**, 3343–3351.

[2] Petrylak DP, Tangen CM, Hussain MH, Lara PN Jr, Jones JA, Taplin ME, Burch PA, Berry D, Moinpour C, Kohli M, et al. (2004). Docetaxel and estramustine compared with mitoxantrone and prednisone for advanced refractory prostate cancer. *N Engl J Med* **351**, 1513–1520.

[3] Emmenegger U, Francia G, Shaked Y, and Kerbel RS (2010). Metronomic chemotherapy: principles and lessons learned from applications in the treatment of metastatic prostate cancer. *Recent Results Cancer Res* **180**, 165–183.

[4] Kerbel RS and Kamen BA (2004). The anti-angiogenic basis of metronomic chemotherapy. *Nat Rev Cancer* **4**, 423–436.

[5] Emmenegger U, Francia G, Chow A, Shaked Y, Kouri A, Man S, and Kerbel RS (2011). Tumors that acquire resistance to low-dose metronomic cyclophosphamide retain sensitivity to maximum tolerated dose cyclophosphamide. *Neoplasia* **13**, 40–48.

[6] Thoenes L, Hoehn M, Kashirin R, Ogris M, Arnold GJ, Wagner E, and Guenther M (2010). *In vivo* chemoresistance of prostate cancer in metronomic cyclophosphamide therapy. *J Proteomics* **73**, 1342–1354.

[7] Ihaka R and Gentleman R (1996). R: a language for data analysis and graphics. *J Comput Graph Stat* **5**, 299–314.

[8] Irizarry RA, Bolstad BM, Collin F, Cope LM, Hobbs B, and Speed TP (2003). Summaries of Affymetrix GeneChip probe level data. *Nucleic Acids Res* **31**, e15.

[9] Gentleman RC, Carey VJ, Bates DM, Bolstad B, Dettling M, Dudoit S, Ellis B, Gautier L, Ge Y, Gentry J, et al. (2004). Bioconductor: open software development for computational biology and bioinformatics. *Genome Biol* **5**, R80.

[10] Huang DW, Sherman BT, and Lempicki RA (2008). Systematic and integrative analysis of large gene lists using DAVID bioinformatics resources. *Nat Protoc* **4**, 44–57.

[11] Fleige S, Walf V, Huch S, Prgomet C, Sehm J, and Pfaffl MW (2006). Comparison of relative mRNA quantification models and the impact of RNA integrity in quantitative real-time RT-PCR. *Biotechnol Lett* **28**, 1601–1613.

[12] Emmenegger U, Shaked Y, Man S, Bocci G, Spasojevic I, Francia G, Kouri A, Coke R, Cruz-Munoz W, Ludeman SM, et al. (2007). Pharmacodynamic and pharmacokinetic study of chronic low-dose metronomic cyclophosphamide therapy in mice. *Mol Cancer Ther* **6**, 2280–2289.

[13] Uysal-Onganer P, Kawano Y, Caro M, Walker MM, Diez S, Darrington RS, Waxman J, and Kypta RM (2010). Wnt-11 promotes neuroendocrine-like differentiation, survival and migration of prostate cancer cells. *Mol Cancer* **9**, 55.

[14] Marchiani S, Tamburrino L, Nesi G, Paglierani M, Gelmini S, Orlando C, Maggi M, Forti G, and Baldi E (2010). Androgen-responsive and -unresponsive prostate cancer cell lines respond differently to stimuli inducing neuroendocrine differentiation. *Int J Androl* **33**, 784–793.

[15] Murray JC, Smith KA, and Thurston G (1989). Flavone acetic acid induces a coagulopathy in mice. *Br J Cancer* **60**, 729–733.

[16] Ny T, Elgh F, and Lund B (1984). The structure of the human tissue-type plasminogen activator gene: correlation of intron and exon structures to functional and structural domains. *Proc Natl Acad Sci USA* **81**, 5355–5359.

[17] Tait JF, Sakata M, McMullen BA, Miao CH, Funakoshi T, Hendrickson LE, and Fujikawa K (1988). Placental anticoagulant proteins: isolation and comparative characterization four members of the lipocortin family. *Biochemistry* **27**, 6268–6276.

[18] Castoldi E and Hackeng TM (2008). Regulation of coagulation by protein S. *Curr Opin Hematol* **15**, 529–536.

[19] Francia G, Shaked Y, Hashimoto K, Sun J, Yin M, Cesta C, Xu P, Man S, Hackl C, Stewart J, et al. (2012). Low-dose metronomic oral dosing of a prodrug of gemcitabine (LY2334737) causes antitumor effects in the absence of inhibition of systemic vasculogenesis. *Mol Cancer Ther* **11**, 680–689.

[20] McVey JH (1999). Tissue factor pathway. *Baillieres Best Pract Res Clin Haematol* **12**, 361–372.

[21] Gouault-Helimann M and Josso F (1979). Initiation *in vivo* of blood coagulation. The role of white blood cells and tissue factor (author's transl). *Nouv Presse Med* **8**, 3249–3253.

[22] Bogdanov VY, Balasubramanian V, Hathcock J, Vele O, Lieb M, and Nemerson Y (2003). Alternatively spliced human tissue factor: a circulating, soluble, thrombogenic protein. *Nat Med* **9**, 458–462.

[23] UniProt Consortium (2012). Reorganizing the protein space at the Universal Protein Resource (UniProt). *Nucleic Acids Res* **40**, D71–D75.

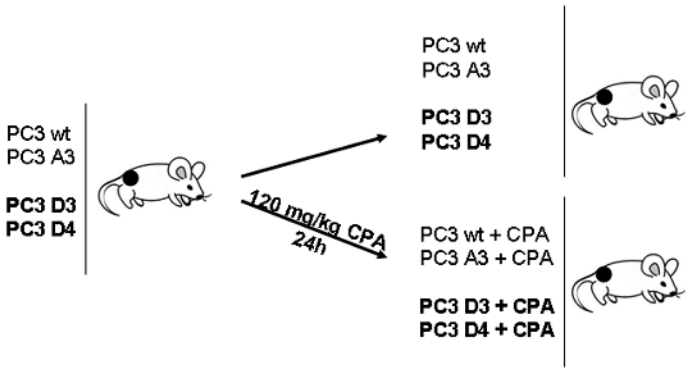

PC3 sublines generated in [6]

PC3 wt	Tumors of parental PC3 cell line (ATCC# CRL1435)
PC3 A3	Tumors of *in vivo* passaged control cell line
PC3 D3	**Tumors of *in vivo* resistant cell line**
PC3 D4	**Tumors of *in vivo* resistant cell line**

Figure W1. Schematic overview of the experimental procedure and cell lines used for the *in vivo* experiments [6].

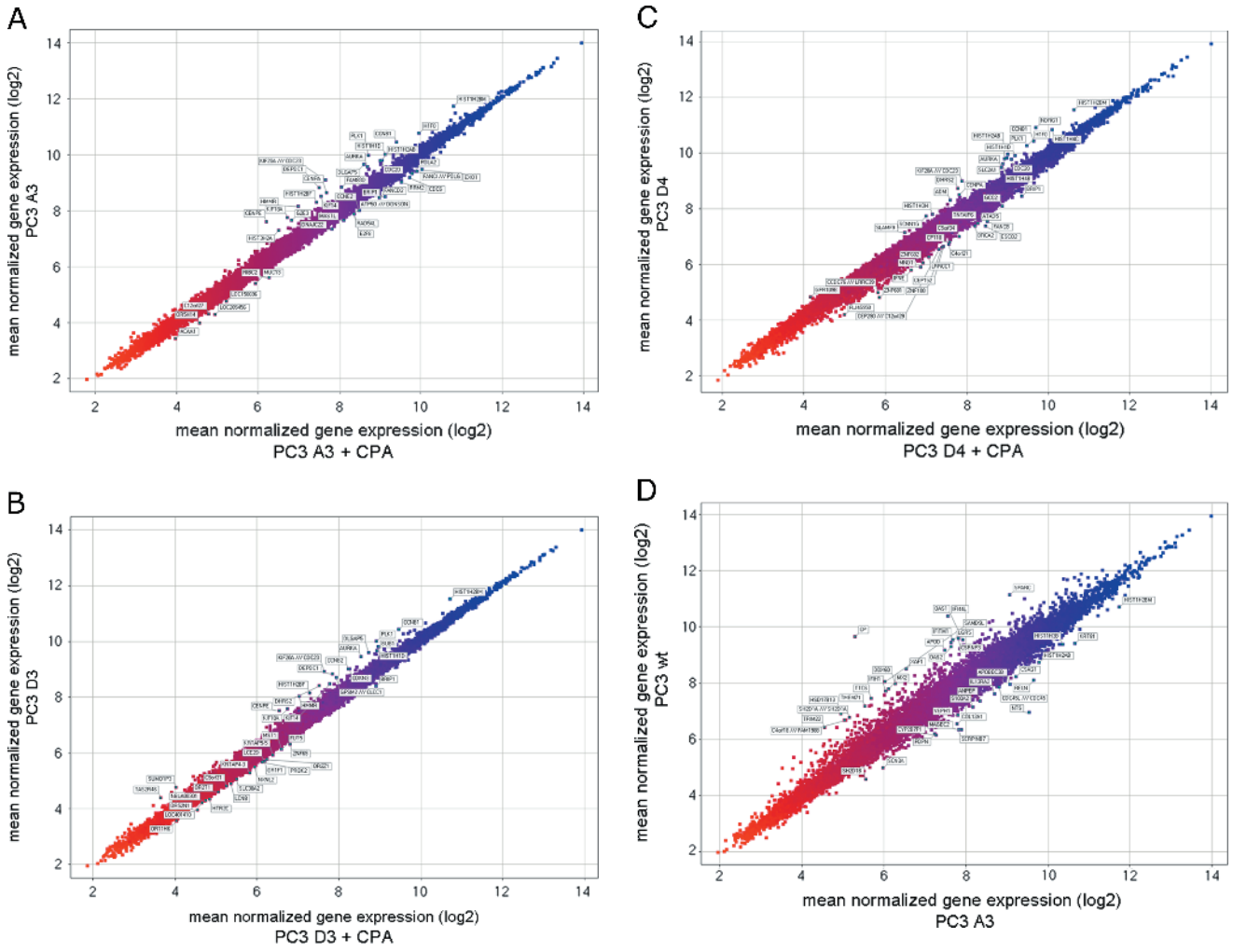

Figure W2. Scatter plot of mean normalized gene expression (log_2) of CPA-treated (24-hour) tumor samples. (A) PC3 A3 + CPA *versus* PC3 A3. (B) PC3 D3 + CPA *versus* PC3 D3. (C) PC3 D4 + CPA *versus* PC3 D4. (D) PC3-wt *versus* PC3 A3.

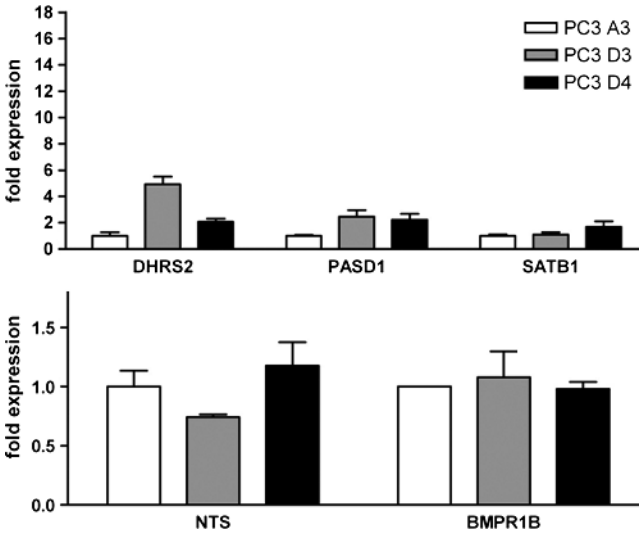

Figure W3. Gene expression of target genes of *in vivo* differentially expressed genes in PC3 sublines cultivated *in vitro* (qPCR, fold expression to control PC3 A3): *DHRS2*, *PASD1*, *SATB1* homeobox 1 (*SATB1*), *NTS*, and *BMPR1B*.

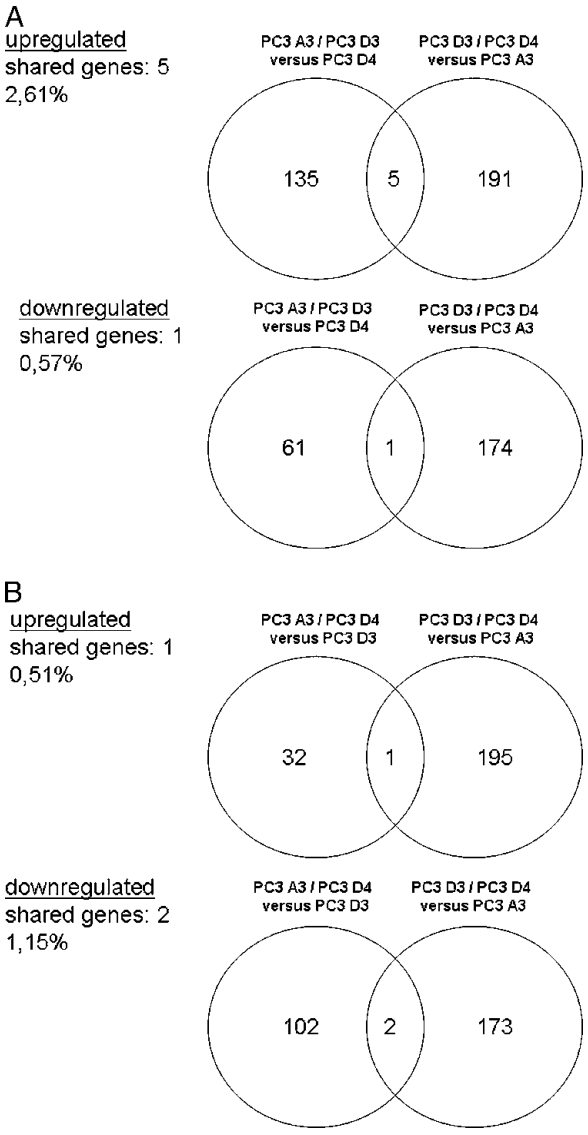

Figure W4. Control experiment. Instead of *in vivo* passaged PC3 A3, one of the resistant tumors, PC3 D3 or PC3 D4, was taken as control and compared to the results, where PC3 A3 tumors served as controls. (A) Venn diagram of PC3 A3 and PC3 D3 *versus* PC3 D4 and PC3 D3 and PC3 D4 *versus* PC3 A3. Cutoff = 0.4. Upper diagram, upregulated genes; lower diagram, downregulated genes. (B) Venn diagram of PC3 A3 and PC3 D4 *versus* PC3 D3 and PC3 D3 and PC3 D4 *versus* PC3 A3. Cutoff = 0.4. Upper diagram, upregulated genes; lower diagram, downregulated genes.